Northumbria
University
NEWCASTLE

Co-immobilization multienzyme nanoreactor with co-factor regeneration for conversion of CO2

Sizhu Ren, Ziyuan Wang, Muhammad Bilal, Yuxiao Feng, Yunhong Jiang, Shiru Jia, Jiandong Cui

PII: S0141-8130(20)32757-4

DOI: https://doi.org/10.1016/j.ijbiomac.2020.03.177

Reference: BIOMAC 15128

To appear in: *International Journal of Biological Macromolecules*

Received date: 6 December 2019

Revised date: 18 March 2020

Accepted date: 20 March 2020

Please cite this article as: S. Ren, Z. Wang, M. Bilal, et al., Co-immobilization multienzyme nanoreactor with co-factor regeneration for conversion of CO2, *International Journal of Biological Macromolecules* (2020), https://doi.org/10.1016/j.ijbiomac.2020.03.177

Co-immobilization multienzyme nanoreactor with co-factor regeneration for conversion of CO2

Sizhu Ren[1], Ziyuan Wang[1], Muhammad Bilal[3], Yuxiao Feng[1], Yunhong Jiang[2*], Shiru Jia[1], Jiandong Cui[1*]

[1]State Key Laboratory of Food Nutrition and Safety, Laboratory of Industrial Fermentation Microbiology, Ministry of Education, Tianjin University of Science and Technology, No 29, 13th, Avenue, Tianjin Economic and Technological Development Area (TEDA), Tianjin 300457, P R China

[2]HBBE, Department of Applied Science, Northumbria University, Newcastle, NE1 8ST, United Kingdom.

[3]School of Life Science and Food Engineering, Huaiyin Institute of Technology, Huaian 223003, China.

[*]Corresponding authors:
Jiandong Cui, E-mail: cjd007cn@163.com, Tel: +86-022-60601598

Yunhong Jiang, E-mail: Yunhong.jiang@northumbria.ac.uk

Abstract

Multienzymatic conversion of carbon dioxide (CO_2) into chemicals has been extensively studied. However, regeneration and reuse of co-factor are still the main problems for the efficient conversion of CO_2. In this study, a nanoscale multienzyme reactor was constrcuted by encapsulating simultaneously carbonic anhydrase (CA), formate dehydrogenase (FateDH), co-factor (NADH), and glutamate dehydrogenases (GDH) into ZIF-8. In the multienzyme reactors, cationic polyelectrolyte (polyethyleneimine, PEI) was doped in the ZIF-8 by dissolving it in the precursors of ZIF-8. Co-factor (NADH) was anchored in ZIF-8 by ion exchange between PEI (positive charge) and co-factor (negative charge), and regenerated through GDH embedded in the ZIF-8, thus keeping high activity of FateDH. Activity recovery of FateDH in the multienzyme reactors reached 50%. Furthermore, the dissolution of CO_2 in the reaction solution was increased significantly by the combination of CA and ZIF-8. As a result, the nanoscale multienzyme reactor exhibited superior capacity for conversion of CO_2 to formate. Compared with free multienzyme system, formate yield was increased 4.6-folds by using the nanoscale multienzyme reactor. Furthermore, the nanoscale multienzyme reactor still retained 50% of its original productivity after 8 cycles, indicating excellent reusability.

Keywords: Carbon dioxide; Bioconversion; Cofactor regeneration; ZIF-8; Multienzyme system

1. Introduction

Nowadays, with the intensification of global warming, capture and conversion of carbon dioxide (CO_2) for the synthesis of chemicals has attracted wide attention[1,2]. Over the past decade, various strategies for CO_2 conversion such as chemical, biological, and enzymatic conversion have been developed [3]. Among various strategies, the enzymatic conversion has been highly noticed due to high yield, high selectivity and specificity, and mild conditions. However, free enzymes often exhibit low stability and poor activity under harsh conditions [4,5]. Enzyme immobilization techniques are well recognized as a common way to improve stability of the enzyme. Generally, the stability of enzyme could be improved by multipoint or multisubunit immobilization due to preventing subunit dissociation, decreasing aggregation, enhancing enzyme rigidification and resistance to inhibitors or chemicals, and et al [6,7]. Recent years, multiple enzyme cascade reactions have a significant role for the production of many compounds at an industrial level because they permit to perform very complex reactions[8-11]. In particular, multi-enzymatic conversion of CO_2 has exhibited good application prospects. Obert and Dave demonstrated for the first time that CO_2 could be reduced continuously to methanol by formate dehydrogenase (FDH), formaldehyde dehydrogenase (FaldDH), and alcohol dehydrogenase (ADH) in the presence of nicotinamide adenine dinucleotide (NADH) [12]. Subsequently, many efforts were performed to realize conversion of CO_2 to methanol by the multi-enzymatic system [13,14]. Although the multi-enzymatic system for CO_2 conversion to chemicals is amazing, the multi-enzymatic system exhibits high cost,

time consuming and low yield due to low solubility of CO_2 in reaction media. At the same time, poor stability and difficulty in recovery of free enzymes in the multi-enzymatic system significantly hampered their industrial-scale applications [15,16]. Furthermore, the regeneration and recycling of cofactor are often a hurdle to implement enzymes at the industrial level [17,18].

To overcome these problems, the co-immobilization strategy of multiple enzymes for CO_2 conversion was developed. For example, FDH, FaldDH, and ADH were successfully co-immobilized in some carriers such as the microcapsule lumen [19], flat-sheet polymeric membranes [20], hollow nanofiber [21], and siliceous mesostructured cellular foams (MCFs) [22]. However, conversion efficiency of CO_2 is still low. Furthermore, once the less stable enzyme is inactivated, all co-immobilized enzymes must be discarded even if some of them fully keep their activity [23,24].

Generally speaking, efficient co-immobilization strategies should include the following principles: Firstly, enzyme denaturation should be minimized in immobilization process. Secondly, the limitation of mass transfer between enzymes and substrates in the co-immobilization system should be very low. Third, it is necessary to realize regeneration of cofactor in the co-immobilization system. Lastly, enhancing the solubility of CO_2 in the reaction solution is the key to improving the conversion of CO_2. Based on the above principles, a co-immobilization multi-enzymatic system for CO_2 conversion with NADH regeneration was constructed, and exhibited the increased methanol productivity [25]. Besides, ionic liquids were used to increase CO_2 solubility in the co-immobilization multi-enzymatic

cascade reaction [26]. Although these examples displayed great potential in increasing the catalysis efficiency of co-immobilization multi-enzymatic system for CO_2 conversion, efficient regeneration and reusing of the cofactor, and increasing the CO_2 solubility in aqueous media are still the biggest challenges in the co-immobilization multi-enzymatic system for CO_2 conversion. Recently, metal-organic frameworks (MOFs) material has been used as an efficient carrier for enzyme immobilization. Compared with other porous materials, MOFs exhibit superior performances on retaining enzyme activity and stability [27-29]. Besides, the recent reports have demonstrated that some MOFs (eg. ZIF-8) possess high capacity of CO_2 capture [30-32]. Furthermore, carbonic anhydrase (CA, EC 4.2.1.1) is a zinc-containing enzyme with same tertiary fold that catalyzes the reversible hydration of carbon dioxide, and can accelerate the hydration of CO_2 [33,34]. Therefore, combination of CA and ZIF-8 by immobilization of CA in ZIF-8 could significantly increase CO_2 solubility in aqueous media. Polyethyleneimine (PEI, a cationic polyelectrolyte) is a polymer containing primary, secondary and tertiary amino groups, having a strong anion exchange capacity, and the capability to chemically react with different moieties on either an enzyme or a support [35]. Furthermore, the co-immobilization of enzymes and cofactors using PEI is one of the preferred ways towards the design of enzyme combi-catalysts for their use in cascade reaction [18,21].

In this study, we propose two immobilization strategies for multi-enzymatic catalysis in ZIF-8, called co- and mix immobilization, as illustrated in Fig. 1. For co-immobilized multienzyme reactor (Co-IMR), CA, glutamate dehydrogenase

(GDH), FateDH (metalloenzymes that catalyse the reversible conversion of formate to carbon dioxide) [36], co-factor (NADH), and PEI were in situ co-encapsulated in the ZIF-8 by co-precipitation method. In the Co-IMR, co-factor (NADH) was anchored in ZIF-8 by ion exchange between PEI (positive charge) and co-factor (negative charge), and regenerated through GDH embedded in the ZIF-8. CA in ZIF-8 accelerated the hydration of CO_2, and FateDH converted CO_2 to formate (Fig. 1a). For mixed immobilized multienzyme reactor (Mix-IMR), On the one hand, CA and FateDH were co-encapsulated in ZIF-8 by co-precipitation method to obtain biocatalyst (enzymes@ZIF-8). On the other hand, PEI, NADH, and GDH were embedded in another ZIF-8 to form NADH regeneration system (NADH@ZIF-8). During catalysis process, enzymes@ZIF-8 and NADH@ZIF-8 were mixed to realize conversion of CO_2 to formate (Fig. 1b). For comparison, Co-IMR without PEI, Co-IMR without GDH, and free multienzyme system (including CA, FateDH, GDH, and NADH) were constructed, respectively. To the best of our knowledge, this is the first attempt to construct the co-immobilized nanoscale multienzyme reactor with co-factor regeneration for CO_2 conversion in ZIF-8. Furthermore, the mechanisms of the co-immobilized multi-enzymatic reaction for CO_2 conversion to formate are discussed.

2.Materials and Methods

2.1 Materials

Formate dehydrogenase from *Candida boidinii* (FateDH, EC.1.2.1.2), p-nitrophenyl acetate (p-NPA), p-nitrophenol, zinc nitrate hexahydrate ($Zn(NO_3)_2 \cdot 6H_2O$), carbonic

anhydrase (CA, EC.4.2.1.1), 2-methylimidazole, and L-glutamic acid were purchased from Sigma-Aldrich Chemical Co., Ltd. Glutamate dehydrogenase (GDH, EC.1.4.1.2) was obtained from Roche Diagnostics GmbH. Fluorescein isothiocyanate (FITC), sulforhodamine 101, Cy5.5-NHS, polyethyleneimine (PEI, MW=70000 g/mole, Cat#E8420), NADH, and NAD^+ were purchased from Beijing Solarbio Science & Techology Co., Ltd. NAD/NADH quantitation Kit was obtained from Suzhou Comin Biotechnology Co., Ltd (NAD-2-Y). Formate (chromatographic grade, Lot #F1817047) was purchased from Aladdin Industrial Corporation. Other chemicals used in this study were of analytical grade.

2.2 Preparation of co-immobilized multienzyme reactor (Co-IMR)

200 μL of glycerol and 800 μL of phosphate buffer solution (0.2 M, pH 7.0) containing 5 mg CA and 15 mg of Fate DH, 15 mg of PEI, 15 mg of NADH, and 15 mg of GDH were mixed. Subsequently, 1 mL zinc nitrate solution (0.4 M) was added into the above mixture solutions, and stirred. Lastly, 10 mL 2-methylimidazole solution (1 M) was added into the mixture, and stirred at room temperature for 30 min. White precipitates were recovered by centrifugation at 12,000 × g for 5 min, and washed for three times by Milli-Q water, and then stored at 4 °C for further use.

2.3 Preparation of mixed immobilized multienzyme reactor (Mix-IMR)

For Mix-IMR, on the one hand, 200 μL of glycerol, 800 μL of phosphate buffer solution (0.2 M, pH 7.0) containing 5 mg CA and 15 mg of Fate DH, and 1 mL zinc nitrate solution (0.4 M) were mixed. Then, 10 mL 2-methylimidazole solution (1 M) was added into the mixture to form enzymes@ZIF-8. On the other hand, 200 μL of

glycerol, 800 μL of phosphate buffer solution (0.2 M, pH 7.0) containing 15 mg of PEI, 15 mg of NADH, and 15 mg of GDH were mixed with 1 mL zinc nitrate solution (0.4 M), and 10 mL 2-methylimidazole solution (1 M) was added into the mixture to obtain NADH@ZIF-8. Both enzymes@ZIF-8 and NADH@ZIF-8 were recovered by centrifugation, and washed for three times by Milli-Q water, and dried. Lastly, enzymes@ZIF-8 and NADH@ZIF-8 were mixed in 1:1 (m/m) to obtain Mixed IMR. For comparison, free multienzyme system (including CA, FateDH, NADH, and GDH), Co-IMR without GDH, and Co-IMR without PEI were prepared, respectively.

2.4 NADH retention efficiency and activity assay

To obtain maximal NADH retention efficiency, effects of PEI concentration (0-20 mg/L) on NADH retention efficiency were investigated. The prepared NADH@ZIF-8 was immersed in 5 mL of phosphate buffer solution (0.2 M, pH 7.0), and incubated at room temperature under 150 rpm shaking for 30 min. The concentration of NADH released into buffer solution from the ZIF-8 was determined by using a NAD/NADH quantitation Kit. The NADH retention efficiency was expressed as the ratio of the NADH retained inside the ZIF-8 to the total amount of NADH initial addition in the solution.

$$\text{NADH retention efficiency (\%)} = \frac{\text{Number of NADH retained in ZIF-8}}{\text{The total amount of NADH addition}} \times 100\% \quad (1)$$

In addition, activities of free CA and immobilized CA were determined by measuring the initial hydrolysis rate of p-NPA to p-nitrophenol at room temperature. Briefly, PBS (10 mM, pH=7.4) containing p-NPA (3 μmol/L) and free CA (3 μg/mL) or

co-immobilized multienzyme nanoreactor (about 1 mg) containing CA (about 3 μg) were mixed to react for 3 minutes. Total reaction process was monitored by measuring the absorbance at 348 nm. CA activity is defined as the hydrolysis of p-NPA per minute. Similar to CA, Fate DH activity was determined by measuring the corresponding initial reduction rate of formic acid. The reaction process was monitored by measuring the absorbance at 340 nm. Fate DH activity was defined as the amount of enzyme needed to reduce 1 μmol formate. Besides, recovered activities of CA and Fate DH in the co-immobilized multienzyme nanoreactors were calculated as given in Eq (2)

$$\text{Recovered activity (\%)} = \frac{\text{CA or FateDH activity in ZIF-8}}{\text{Total free CA or FateDH activity used for nanoreactor}} \times 100\% \quad (2)$$

2.5 Characterization

Scanning electron microscope (SEM, Hitachi S4800) was used to observe the morphologies of ZIF-8. FT-IR measurements (NEXUS870 infrared spectrometer) were conducted in the region of 400-4000 cm^{-1}. Powder X-ray diffraction (PXRD) patterns were recorded using a X-ray powder diffraction (D/Max-2500 diffractometer, Shimadzu, Japan). Energy-dispersive spectrometer (EDS) (S2 Ranger, Bruker, Germany) was used to determine elemental composition of Co-IMR. In order to characterize the distribution of enzymes in ZIF-8, CA, Fate DH and GDH were labeled with fluoresceinisothiocyanate (FITC), sulforhodamine 101, and Cy 5.5-NHS dye, respectively. The labeled CA, FateDH and GDH were used to prepare Co-IMR. Confocal laser scanning microscopy (CLSM) was taken by Leica TCS SP5

microscope (Leica Camera AG, Germany). The laser caused excitation of FITC and sulforhodamine 101, and Cy 5.5-NHS at 488, 543, and 673 nm, and emitted fluorescent light was detected at 545, 605, and 707 nm.

2.6 Effects of temperatures and pH on immobilized enzymes and free enymes

Effects of temperature on activities of free CA and Fate DH, immobilized CA and Fate DH were investigated by adding the enzyme samples into the substrate solution at different temperatures (20-60 °C) for 30 min. Effects of pH on activities of free CA and Fate DH, immobilized CA and Fate DH were also determined by adding the enzyme samples into the substrate solution with different pH (4-10) at 30 °C for 30 min. The activity of CA and Fate DH was determined as mentioned in activity assay section.

2.7 Conversion CO_2 to formate

For co-immobilized multienzymes, CO_2 gas was introduced into PBS (10 mM, pH=7.4) containing 10 mM L-glutamate for 30 min. Then, 50 mg co-immobilized multienzymes (including 0.8 U/mg Fate DH, 1.6 U/mg CA, and 22 U/mg GDH, and 40 mg/mg) were added into the mixture to react for 1 h. For free multienzyme system, CO_2 gas was introduced into a reaction mixture containing 10 mM L-glutamate and the free enzymes (including 4 U Fate DH, 80 U CA, and 120 U GDH) for 30 min. Then, NADH (2 g) was added to initiate the reaction. After 1 h, 20 μL of sample containing formate was taken from the reaction mixture and detected by using high-performance liquid chromatography (HPLC) with a BIO-RAD organic acid analysis column (HPX-87H Ion Exclusion Column,300×7.8 mm) and a ultraviolet

detector at 210 nm. The mobile phase was 5 mM H_2SO_4 with its flow rate of 0.6 mL/min. The column temperature was kept at 65 °C during the analysis. A calibration curve for formate was prepared by employing the known concentrations of formate that ranged from 10 to 200 μg/mL.

2.8 Reusability tests

Reusability of Co-IMR was evaluated by measuring formate yield during repeated usages. CO_2 gas was introduced into the mixture solution containing 10 mM L-glutamate and 50 mg Co-IMR for 1 h. Subsequently, Co-IMR was recovered from reaction mixture by filtration, and washed for three times, and then suspended with a fresh reaction solutions. The reaction solutions were gathered from all the 8 cycles. Formate yield was determined by HPLC.

3.Results and discussion

3.1 Preparation and characterization of nanoscale multienzyme reactor

The previous reports have demonstrated that enzymes could be encapsulated in situ by co-precipitation in the ZIF-8 [37,38]. The formed ZIF-8 protective shell around immobilized enzymes could prevent the leakage of enzyme molecules from ZIF-8 [39,40]. Enzyme cofactors play a major role in cofactor-dependent enzymes. However, the cofactor recycling is often a hurdle to implement enzymes at the industrial level. Therefore, the preparation of biocatalysts co-immobilizing cofactors and enzymes onto the same material is necessary to perform chemical reactions without exogeneous addition of cofactors[17,18]. Recently, self-sufficient heterogeneous

biocatalysts integrating enzymes and cofactors within the same porous microbead were successfully prepared, in this biocatalysts, the enzymes and PEI were irreversibly bound to the solid surface, and the negative charged cofactors were reversibly adsorbed to the PEI through ion-exchange interactions [18]. These results suggested that both the co-immobilization of enzymes and cofactors on/in the same supporter were an efficient approach for improving catalytic performances of cofactor-dependent enzymes. In this study, PEI was doped in the ZIF-8 by dissolving it in the precursors of ZIF-8. It was expected that the ion exchange between positively charged PEI and negatively charged NADH will enable tethering of NADH molecule in the ZIF-8, thus decreasing leakage of NADH from the ZIF-8 and improving regeneration of NADH.

To confirm the feasibility of the retention of NADH in the ZIF-8 by ion exchange, effects of PEI concentration on the retention of NADH in the ZIF-8 were investigated. The results were shown in Fig. 2. No NADH was detected in ZIF-8 when PEI was not introduced in ZIF-8. However, when the concentration of PEI was increased from 0 to 15 mg/mL, the retention efficiency of NADH in ZIF-8 increased. At low PEI concentration (5 mg/L), the retention efficiency of NADH in ZIF-8 was 79%. This may be the fact that the ionizable groups provide by PEI are not enough to provide strong NADH-PEI interactions, thus causing leakage of NADH from ZIF-8. With increasing the PEI concentrations from 5 to 15 mg/mL, the interactions between NADH and PEI were strengthened. As a result, retention efficiency of NADH was significantly increased, and the maximum retention efficiency of NADH reached

93.46% when PEI concentration was 15 mg/L. However, a further increase in the PEI concentration (20 mg/L) resulted in decrease in NADH retention efficiency. The decreased NADH retention efficiency at high PEI concentration could be due to shape changes of the ZIF-8. As shown in Fig. S1, at low PEI concentration (5-15 mg/L), ZIF-8 showed homogeneous and intact structure. However, when PEI concentration was increased to 20 mg/L, ZIF-8 with broken structure was observed. TEM images further confirmed this phenomenon (Fig. S2). The results could be due to strong electrostatic repulsive force among PEI molecules in ZIF-8, thus causing NADH leakage. Analysis of EDS showed that signals for P element was observed in the ZIF-8 with tethering NADH (Fig. S3). The results revealed that NADH was successfully retained in the ZIF-8 because only NADH contains P element. Besides, SEM images showed that no significant changes were observed for the morphology of the pure ZIF-8, Co-IMR, Mix-IMR, Co-IMR without PEI, and Co-IMR without GDH (Fig. 3). The result indicated that the presence of enzyme proteins could not directly affect the morphology of ZIF-8. Furthermore, PXRD measurements (Fig. 4a) indicated that the crystal structure and crystallinity of the pure ZIF-8, Co-IMR, Mix-IMR, Co-IMR without PEI, and Co-IMR without GDH remained unchanged, further confirming that the shape of ZIF-8 was not affected by enzyme proteins. Similar results were also observed in previous reports [27,41]. In addition, FTIR spectrum revealed that the characteristic bands at 998 cm^{-1} and 1470 cm^{-1} in all samples were ascribed to the stretching and plane bending in imidazole ring [42], indicating the formation of ZIF-8 (Fig. 4b). The absorption peaks observed at 3376

cm^{-1} and 1568 cm^{-1} in the Co-IMR was attributed to be the stretching vibration and deformation vibration of N-H in CA, Fate DH, and GDH [43]. The bands at 1640 cm^{-1} to 1660 cm^{-1} are assigned to amide I of proteins stretching [41], further indicating the presence of CA, Fate DH, and GDH. To further confirm presence of CA, Fate DH, and GDH in ZIF-8, different fluorescently labeled enzyme molecules (CA prelabeled with FITC, FateDH prelabeled with sulforhodamine 101, and GDH prelabeled with Cy5.5-NHS) were synthesized, and used to prepare the immobilized enzymes, respectively. The confocal microscope images were showed in Fig. 5. ZIF-8 with CA only emitted green fluorescence (FITC label) (Fig. 5a), ZIF-8 with Fate DH only displayed red fluorescence (sulforhodamine 101 label) (Fig. 5b), and ZIF-8 with GDH only exhibited blue fluorescence (Cy5.5-NHS label) (Fig. 5c). However, Co-IMR with CA, Fate DH, and GDH yielded pink fluorescence (the mix of red, blue and green is pink)(Fig. 5d). This result further confirmed that CA, Fate DH, and GDH were co-encapsulated in ZIF-8. Furthermore, it was found that immobilization efficiency of CA and Fate DH in the co-IMR was 74.3% and 68.2%, respectively. Compared with co-IMR, CA and Fate DH in the Mix-IMR exhibited similar immobilization efficiency, reaching 71.8% and 65.7.%, respectively.

3.2 The catalytic activity of the nanoscale multienzyme reactor

In the Co-IMR, Fate DH play an important role in the reduction of CO_2 to formate. Therefore, effects of Fate DH concentration on the activity recovery in the Co-IMR was investigated. At this case, CA concentration was still maintained at 5 mg/mL. Fate DH concentration was varied from 5 mg/mL to 15 mg/mL. The results were

shown in Fig. S4. The activity recovery of Fate DH was increased with increasing Fate DH concentration. The maximum activity recovery (52%) was obtained when Fate DH concentration was 10 mg/mL. However, a further increase of Fate DH concentration (15 mg/mL) decreased activity recovery of Fate DH. The phenomenon was observed in the previous reports [13,20]. In addition, optimum pH and temperature were investigated for the immobilized enzymes and free enzymes. It was found that optimum temperature of all enzyme samples was 30 °C (Fig. S5). Furthermore, both immobilized CA and immobilized Fate DH maintained relatively high activity over a wide range of temperature (30-60 °C), indicating that immobilized enzymes had higher thermal stability than free enzymes. The enhanced thermostability can be attributed to confinement of enzymes in ZIF-8 microenvironments, preventing subunit dissociation and protein unfolding [4, 7, 16] . Besides, maximum activities of both the free and immobilized Fate DH were observed at pH 7.0. The optimum pH of free and immobilized CA was at 8.0 (Fig. S6). Furthermore, the pH activity profiles of immobilized enzymes were broader than those of the free enzymes.

3.3 Conversion of CO_2 into formate

In addition, conversion of CO_2 into formate was performed in batch mode. The results showed that no formate was detected when the Co-IMR without PEI and Co-IMR without GDH was used as catalyst (data not shown). This result may be due to the loss of NADH from ZIF-8. In contrast, CO_2 was successfully reduced into formate by using free multienzyme system, Co-IMR, and Mix-IMR (Fig. S7, Fig. S8,

and Fig. S9). The results showed that NADH was regenerated by GDH in free multienzyme system, Co-IMR, and Mix-IMR. The formate yields increased at 40 min during batch operation mode, but they retained a constant value as the reaction time prolonged during the 1 h reaction for all systems (Fig. S10). The formate yield using free multienzyme system was higher than that of the Co-IMR and Mix-IMR throughout the 1 h reaction process. However, it was found that the formate yield using Co-IMR was 5 folds compared with Mix-IMR (Fig. 6b). There are some possible reasons for this unexpected result. First, compared with Co-IMR, there may be high mass transfer resistance for Mix-IMR between NADH and Fate DH. Therefore, the substrate/NADH could not rapidly access Fate DH in the Mix-IMR. Second, free NADH transfer between enzymes@ZIF-8 and NADH@ZIF-8 in Mix-IMR might be inefficient due to high mass transfer resistance, thus causing low Fate DH activity. It is worth noting that although the formate yield using Co-IMR for the first cycle in batch mode was lower than free multienzyme system, Co-IMR exhibited excellent reusability. As shown in Fig. 6a, the Co-IMR still retained 50% of its original productivity after 8 reusing cycles. However, the Mix-IMR lost productivity after 2 reusing cycles (data not shown). Furthermore, compared with free multienzyme system, a 4.6-fold increase in total cumulative formate yield was obtained after 8 reusing cycles (Fig. 6b). Formate yield reached 13.8 mM. The yield was compared with previous reports (Table S1). Addo et al. achieved successfully the reduction of CO_2 to formate using Fate DH in the electrochemical NADH regeneration. Formate yield reached 0.7 mM after 25 hours [44]. Srikanth et al.

produced 8.9 mM of formate by using a bioelectrochemical system including Fate DH and NADH regeneration at 3 hours [45]. CO_2 was reduced to formate with Fate DH during electrochemical NADH regeneration. 2.4 mM of formate was produced after 5 hours [46]. Lee et al. immobilized Fate DH and NADH on polydopamine film on a glassy carbon electrode for the reduction of CO_2 to formate. After 24 hours 16 mM of formate was produced [47]. Recently, the similar results were also reported [48,49]. In this study, the reduction of CO_2 to formate was accelerated by the combination of CA and ZIF-8. Meanwhile, regeneration and reuse of co-factor were realized in the Co-IMR. Furthermore, the confinement effect of nanoscale ZIF-8 also enhanced the stability of the multienzyme system significantly. Therefore, CO_2 was reduced efficiently to the formate by the Co-IMR.

4. Conclusion

In summary, we have successfully constructed nanoscale multienzyme reactors by co-immobilization of CA and Fate DH in ZIF-8 for conversion CO_2 to formate. In the nanoscale multienzyme reactors, NADH was tethered in ZIF-8 by using ion exchange between positively charged PEI and negatively charged co-factor, and regenerated through GDH embedded in the ZIF-8, thus keeping high activity of FateDH. Therefore, the nanoscale multienzyme reactor exhibited superior capacity for conversion of CO_2 to formate. Compared with free multienzyme system, formate yield was increased 4.6-folds by using the nanoscale multienzyme reactor. This study provides an efficient strategy for designing co-immobilized multi-enzymatic cascade

system for conversion of CO_2 to high value-added chemicals.

Acknowledgments

This work is partially supported by the Science and Technology Program of Tianjin, China (project no.18PTSYJC00140), and the National Natural Science Foundation of China (project no. 21676069). Dr. J. D. Cui also thanks supports from the Key Projects of Tianjin Natural Science Foundation, China (project no. 19JCZDJC38100), the Program for Hundreds of Outstanding Innovative Talents in Hebei province (III) under the grant number of SLRC2017036.

Reference

[1] T. Baran, S. Wojtyła, A. Dibenedetto, M. Aresta, W. Macyk, Zinc sulfide functionalized with ruthenium nanoparticles for photocatalytic reduction of CO_2. Appl. Catal. B-Environ. 178(2015)170-176.

[2] S. Kim, K. K. Min, H. L. Sang, S. Yoon, K. D. Jung, Conversion of CO_2 to formate in an electroenzymatic cell using *Candida boidiniiformate* dehydrogenase. J. Mol. Catal. B-Enzym. 102(2014) 9-15.

[3] J. H. Jiang, A. Wieckowski, Prospective direct formate fuel cell. Electrochem. Commun. 18(2012) 41-43.

[4] C. Garcia-Galan, A. Berenguer-Murcia, R. Fernandez-Lafuente, R. C. Rodrigues, Potential of different enzyme immobilization strategies to improve enzyme performance. Adv Synth Catal. 353(2011)2885-2904.

[5] O. Barbosa, C. Ortiz, Á. Berenguer-Murcia, R. Torres, R. C. Rodrigues, R. Fernandez-Lafuente, Strategies for the one-step immobilization–purification of enzymes as industrial biocatalysts. Biotechnol Adv. 33(2015) 435-456.

[6] D. A. Cowan, R. Fernandez-Lafuente, Enhancing the functional properties of thermophilic enzymes by chemical modification and immobilization. Enzyme Microb. Tech. 49(2011) 326-346.

[7] R. Fernandez-Lafuente, Stabilization of multimeric enzymes: strategies to prevent subunit dissociation. Enzyme Microb. Tech. 45(2009)405-418.

[8] S. Z. Ren, C. H. Li, X. B. Jiao, S. R. Jia, Y. J. Jiang, M. Bilal, J. D. Cui, Recent progress in multienzymes co-immobilization and multienzyme system applications.

Chem. Eng. J. 373 (2019) 1254-1278.

[9] C. Schmid-Dannert, F. Lopez-Gallego, Advances and opportunities for the design of self-sufficient and spatially organized cell-free biocatalytic systems. Curr. Opin Chem Biol. 49(2019)97-104.

[10] A. Benitez-Mateos, M. L. Contente, S. Velasco-Lozano, F. Paradisi, F. Lopez-Gallego, Self-sufficient flow-biocatalysis by coimmobilization of pyridoxal 5′-phosphate and ω-transaminases onto porous carriers. ACS Sustainable Chem Eng. 6(2018) 13151-13159.

[11] A. H. Orrego, F. Lopez-Gallego, A. Espaillat, F. Cava, J. M. Guisan, J. Rocha-Martin. One-step synthesis of α-Keto acids from racemic amino acids by a versatile immobilized multienzyme cell-free system. ChemCatChem, 10(2018)3002-3011.

[12] I. Tsujisho, M. Toyoda, Y. Amao, Photochemical and enzymatic synthesis of formic acid from CO_2 with chlorophyll and dehydrogenase system. Catal. Commun. 7(2006) 173-176.

[13] R. Obert, B. C. Dave, Enzymatic conversion of carbon dioxide to methanol: enhanced methanol production in silica sol-gel matrices. J. Am. Chem. Soc. 121(1999) 12192-12193.

[14] R. Cazelles, J. Drone, F. Fajila, O.Ersen, S. Moldovan, A. Galarneau, Reduction of CO_2 to methanol by a polyenzymatic system encapsulated in phospholipids-silica nanocapsules. New. J. Chem. 37(2013) 3721-3730.

[15] P. Hanachi, F. Jafary, S. Motamedi, Immobilization of the alkaline phosphatase

on collagen surface via cross-linking method. Iran. J. Biotechnol. 13(2015) 32-38.

[16] Z. Lian, Y. Fang, E. Joseph, Q. Wang, J. L. Li, S. Banerjee, C. Lollar, X. Wang, H.C. Zhou, Enzyme-MOF (metal-organic framework) composites. Chem. Soc. Rev. 46(2017) 3386-3401.

[17] A. Benitez-Mateos, E. S. Sebastian, N. Rios-Lombardia, F. Moris, J. Gonzalez-Sabin, F. Lopez-Gallego. Asymmetric reduction of prochiral ketones by using self-sufficient heterogeneous biocatalysts based on NADPH-dependent ketoreductases. Chem Eur J, 23 (2017) 16843-16852.

[18] S. Velasco-Lozano, A. Benites-Nateos, F. Lopez-Gallego. Co-immobilized phosphorylated cofactors and enzymes as self-sufficient heterogeneous biocatalysts for chemical processes. Angew Chem Int Edit, 56 (2017) 771-775.

[19] L. Wang, Z. Li, J. F. Shi, H. Wu, Z. Y. Jiang, W. Y. Zhang, X. K. Song, Q.H. Ai, Bioinspired approach to multienzyme cascade system construction for efficient carbon dioxide reduction. ACS Catal. 4(2014) 962-972.

[20] J. Luo, A. S. Meyer, R. V. Mateiu, M. Pinelo, Cascade catalysis in membranes with enzyme immobilization for multi-enzymatic conversion of CO_2 to methanol. New Biotechnol. 32(2015)319-372.

[21] X. Ji, Z. G. Su, G. H. Ma, S. P. Zhang, Tethering of nicotinamide adenine dinucleotide inside hollow nanofibers for high-yield synthesis of methanol from carbon dioxide catalyzed by coencapsulated multienzymes. ACS Nano. 9(2015) 4600-4610.

[22] P. S. N. Zadeh, J. Muschiol, Y. H. Huang, S. B. Sigurdardottir, N. V. Solms, A. E.

Daugaard, J. Wei, J. Q. Luo, B. H. Xu, S. J. Zhang, M. Pinelo, Förster resonance energy transfer study of the improved biocatalytic conversion of CO_2 to formaldehyde by co-immobilization of enzymes in siliceous mesostructured cellular foams. ACS Catal. 8(2018) 7251-7260.

[23] S. Arana-Peña, C. Mendez-Sanchez, N.S. Rios, C. Ortiz, L.R.B. Gonçalves, R. Fernandez-Lafuente, New applications of glyoxyl-octyl agarose in lipases co-immobilization: Strategies to reuse the most stable lipase. Inter J. Biol Macromol. 131(2019)989-997.

[24] S. Peirce, J. J. Virgen-Ortíz, V. G. Tacias-Pascacio, N. Rueda, R. Bartolome-Cabrero, L. Fernandez-Lopez, M. E. Russo, A. Marzocchella, R. Fernandez-Lafuente, Development of simple protocols to solve the problems of enzyme coimmobilization. Application to coimmobilize a lipase and a β-galactosidase RSC Advances, 6(2016)61707-61715.

[25] R. K. Singh, R. Singh, D. Sivakumar, S. Kondaveeti, T. Kim, J. L. Li, B. H. Sung, B. K. Cho, D. R. Kim, S. C. Kim, V. C. Kalia, Y. H. P. J. Zhang, H. M. Zhao, Y. C. Kang, J. K. Lee, Insights into cell-free conversion of CO_2 to chemicals by a multienzyme cascade reaction. ACS Catal. 8(2018) 11085-11093.

[26] Z. Zhang, J. Muschiol, Y. H. Huang, S. B. Sigurdardottir, N. V. Solms, A. E. Daugaard, J. Wei, J. Q. Luo, B. H. Xu, S. J. Zhang, M. Pinelo, Efficient ionic liquid-based platform for multi-enzymatic conversion of carbon dioxide to methanol. Green Chem. 20(2018) 4339-4348.

[27] P. Li, S. Y. Moon, M. A. Guelta, S. P. Harvey, J. T. Hupp, O. K. Farha,

Encapsulation of a nerve agent detoxifying enzyme by a mesoporous zirconium metal-organic framework engenders thermal and long-term stability. J. Am. Chem. Soc. 138(2016)8052-8055.

[28] X. Wu, M. Hou, J. Ge, Metal–organic frameworks and inorganic nanoflowers: a type of emerging inorganic crystal nanocarrier for enzyme immobilization. Catal. Sci. Technol. 5(2015) 5077-5085.

[29] J. D. Cui, S. Z. Ren, B. T. Sun, S. R. Jia, Optimization protocols and improved strategies for metal-organic frameworks for immobilizing enzymes: Current development and future challenges. Coordin. Chem. Rev. 370(2018) 22-41.

[30] W. Zheng, R. Ding, K. Yang, Y. Dai, X. M. Yan, G. H. He, ZIF-8 nanoparticles with tunable size for enhanced CO_2 capture of Pebax based MMMs. Sep. Purif. Technol. 214(2019) 111-119.

[31] J. S. Lainez, B. Zornoza, C. Tellez, J. Coronas, Asymmetric polybenzimidazole membranes with thin selective skin layer containing ZIF-8 for H_2/CO_2 separation at pre-combustion capture conditions. J. Membrane. Sci. 563(2018) 427-434.

[32] M. Mohamedali, H. Ibrahim, A. Henni, Incorporation of acetate-based ionic liquids into a zeolitic imidazolate framework (ZIF-8) as efficient sorbents for carbon dioxide capture. Chem. Eng. J. 334(2018) 817-828.

[33] B. K. Shanbhag, B. Y. Liu, J. Fu, V. S. Haritos, L. Z. He, Self-assembled enzyme nanoparticles for carbon dioxide capture. Nano Lett. 16(2016) 3379-3384.

[34] I. Iliuta, M. Iliuta, Investigation of CO_2 removal by immobilized carbonic anhydrase enzyme in a hollow-fiber membrane bioreactor. AICHE J. 63(2017)

2996-3007.

[35] J. J. Virgen-Ortiz, J. C. S. dos Santos, A. Berenguer-Murcia, O. Barbosa, R. C. Rodrigues, R. Fernandez-Lafuente. Polyethylenimine: A very useful ionic polymer in the design of immobilized enzyme biocatalyst. J. Mater. Chem B. 5(2017) 7461-7490.

[36] G. Dong, U. Ryde, Reaction mechanism of formate dehydrogenase studied by computational methods. J. Biol. Inorg. Chem. 23(2018) 1243-1254.

[37] S. Zhang, M. Du, P. J. Shao, L. D. Wang, J. X. Ye, J. Chen, J. M. Chen, Carbonic anhydrase enzyme-MOFs composite with a superior catalytic performance to promote CO_2 absorption into tertiary amine solution, Environ. Sci. Technol. 52(2018) 12708-12716.

[38] S. Ren, C. H. Li, Z. L. Tan, Y. Hou, S. R. Jia, J. D. Cui, Carbonic anhydrase@ZIF-8 hydrogel composite membrane with improved recycling and stability for efficient CO_2 capture. J. Agric. Food Chem. 67(2019) 3372-3379.

[39] P. Li, Q. S. Chen, T. C. Wang, N. A. Vermeulen, B. L. Mehdi, A. Dohnalkova, N. D. Browning, D. K. Shen, R. Anderson, D. A. Gomez-Gualdron, F. M. Cetin, J. Jagiello, A. M. Asiri, J. F. Stoddart, O. K. Farha, Hierarchically engineered mesoporous metal-organic frameworks toward cell-free immobilized enzyme systems. Chem. 4(2018) 1022-1034.

[40] R. J. Drout, L. Robison, O. K. Farha, Coordin. Catalytic applications of enzymes encapsulated in metal-organic frameworks. Coordin. Chem. Rev. 381(2019) 151-160.

[41] J. D. Cui, Y. X. Feng, T. Lin, Z. L. Tan, C. Zhong, S. R. Jia, Mesoporous metal–organic framework with well-defined cruciate flower-like morphology for

enzyme immobilization. ACS Appl. Mater. Interfaces. 9(2017) 10587-10594.

[42] W. Yang, H. Chen, Z. Yun, H. Fu, M. Z. Liu, X. L. Li, Preparation of graphene nano-sheet bonded PDA/MOF microcapsules with immobilized glucose oxidase as a mimetic multi-enzyme system for electrochemical sensing of glucose. J. Mat. Chem. B. 4(2016) 3695-3702.

[43] N. Mahmood, M. Islam, A. Hameed, S. Saeed, A. Nawaz, Polyamide-6-based composites reinforced with pristine or functionalized multi-walled carbon nanotubes produced using melt extrusion technique, J. Compos Mater. 48(2014) 1197-1207.

[44] P. K. Addo, R.L. Arechederra, A. Waheed, J. D. Shoemaker, W. S. Sly, S. D. Minteer, Methanol production via bioelectrocatalytic reduction of carbon dioxide: role of carbonic anhydrase in improving electrode performance, Electrochem. Solid-State Lett. 14(2011) E9-E13.

[45] S. Srikanth, M. Maesen, X. Dominguez-benetton, K. Vanbroekhoven, Enzymatic electrosynthesis of formate through CO_2 sequestration/reduction in a bioelectrochemical system (BES), Bioresour. Technol. 165(2014), 350-354.

[46] S. Kim, G. Chung, S. Kim, G. Vinothkumar, S. Yoon, K. Jung, Electrochemical NADH regeneration and electroenzymatic CO_2 reduction on Cu nanorods/glassy carbon electrode prepared by cyclic deposition, Electrochim. Acta. 210(2016) 837-845.

[47] S. Y. Lee, S. Y. Lim, D. Seo, J. Lee, T. D. Chung, Light-driven highly selective conversion of CO_2 to formate by electrosynthesized enzyme/cofactor thin film electrode, Adv. Energy Mater. 6(2016) 1-8.

[48] Y. Li, L. Y. Wen, T, W. Tan, Y, Q. Lv, Sequential co-immobilization of enzymes in metal-organic frameworks for efficient biocatalytic conversion of adsorbed CO_2 to formate, Front. Bioeng. Biotechnol. 7(2019) 394.

[49] R. Barin, D. Biria, S. Rashid-Nadimi, M. A. Asadollahi, Investigating the enzymatic CO2 reduction to formate with electrochemical NADH regeneration in batch and semi-continuous operations, Chem. Eng. Process, 140(2019) 78-84.

Figure legend

Fig. 1 Preparation of catalysts including Co-IMR and Mix-IMR.

Fig. 2 Effects of different concentrations of PEI on NADH retention efficiency in the ZIF-8.

Fig. 3 (a). ZIF-8 support, (b). Co-IMR, (c). Mix-IMR, (d). Co-IMR without PEI, (e). Co-IMR without GDH.

Fig. 4 PXRD spectra (a) of ZIF-8, Co-IMR, Mix-IMR, Co-IMR without PEI, and Co-IMR without GDH; FTIR spectra (b) of ZIF-8, Co-IMR, Mix-IMR, Co-IMR without PEI, and Co-IMR without GDH.

Fig. 5 CLSM imaging in dark-field of Co-IMR. (a). FITC-CA (Green), (b). Sulforhodamine 101-FateDH (Solferino), (c). Cy5.5-NHS-GDH (Blue, after adjusting the laser), (d). Three enzymes co-immobilization by multiple channel mode..

Fig. 6 Reusability (a) of Co-IMR; (b) Cumulative formate yield using different catalysts.

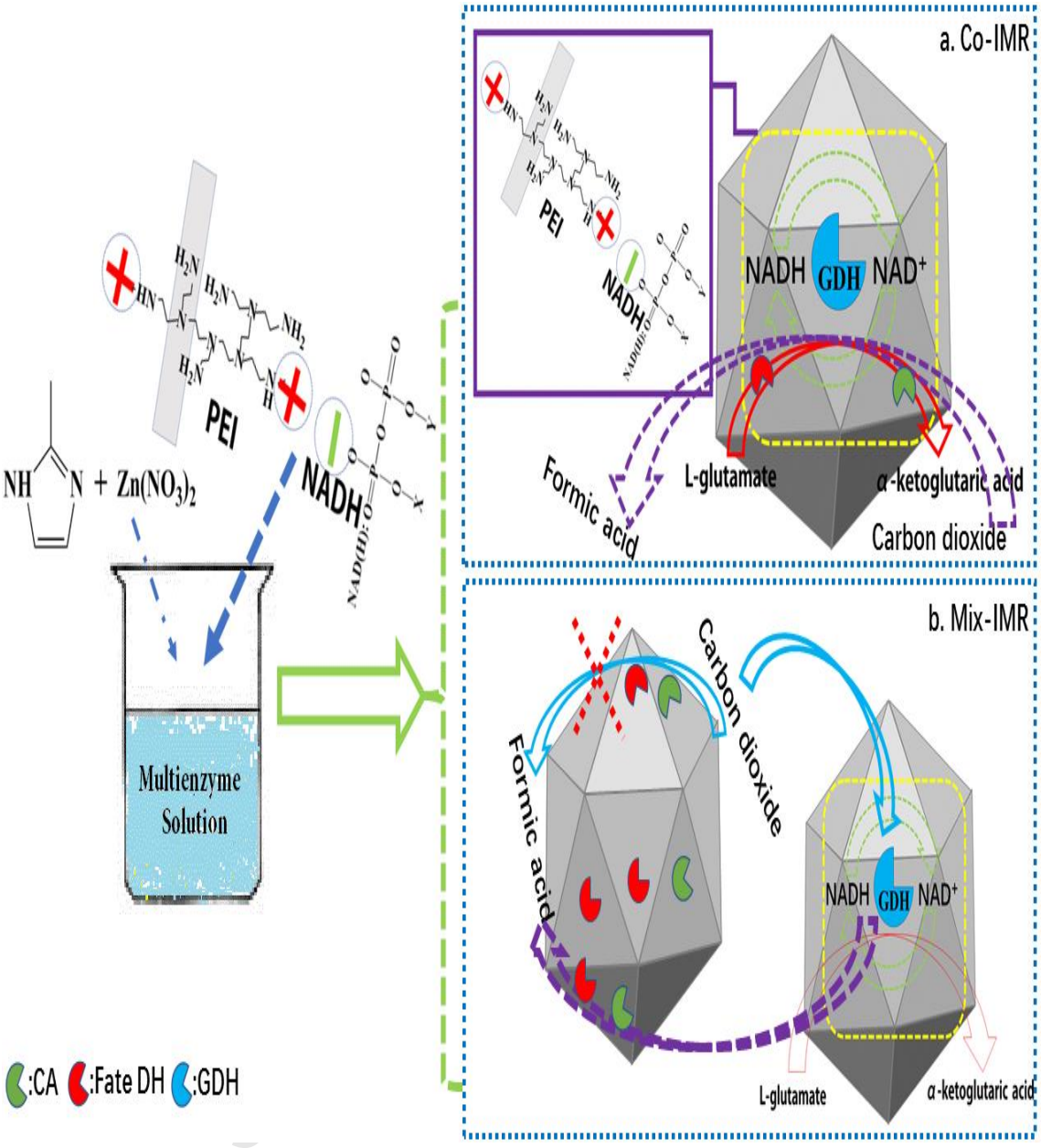
a. Co-IMR
PEI
NADH
NADH GDH NAD+
Formic acid
L-glutamate
α-ketoglutaric acid
Carbon dioxide
NH N + Zn(NO3)2
Multienzyme Solution
b. Mix-IMR
Carbon dioxide
Formic acid
NADH GDH NAD+
L-glutamate
α-ketoglutaric acid
:CA :Fate DH :GDH

Fig.1

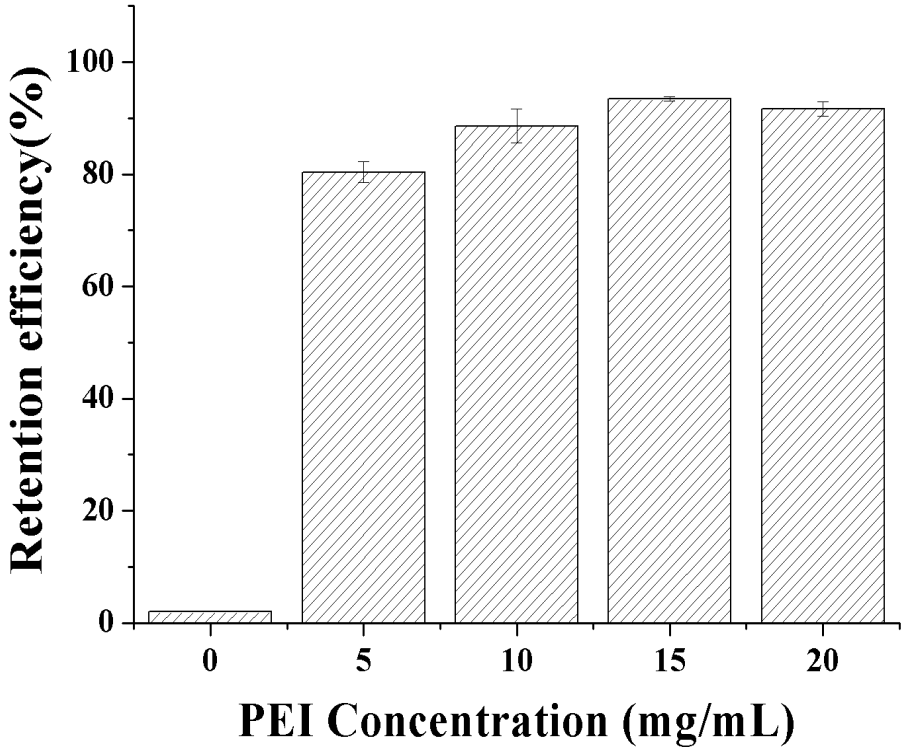
Retention efficiency(%)
100
80
60
40
20
0
0
5
10
15
20
PEI Concentration (mg/mL)

Fig.2

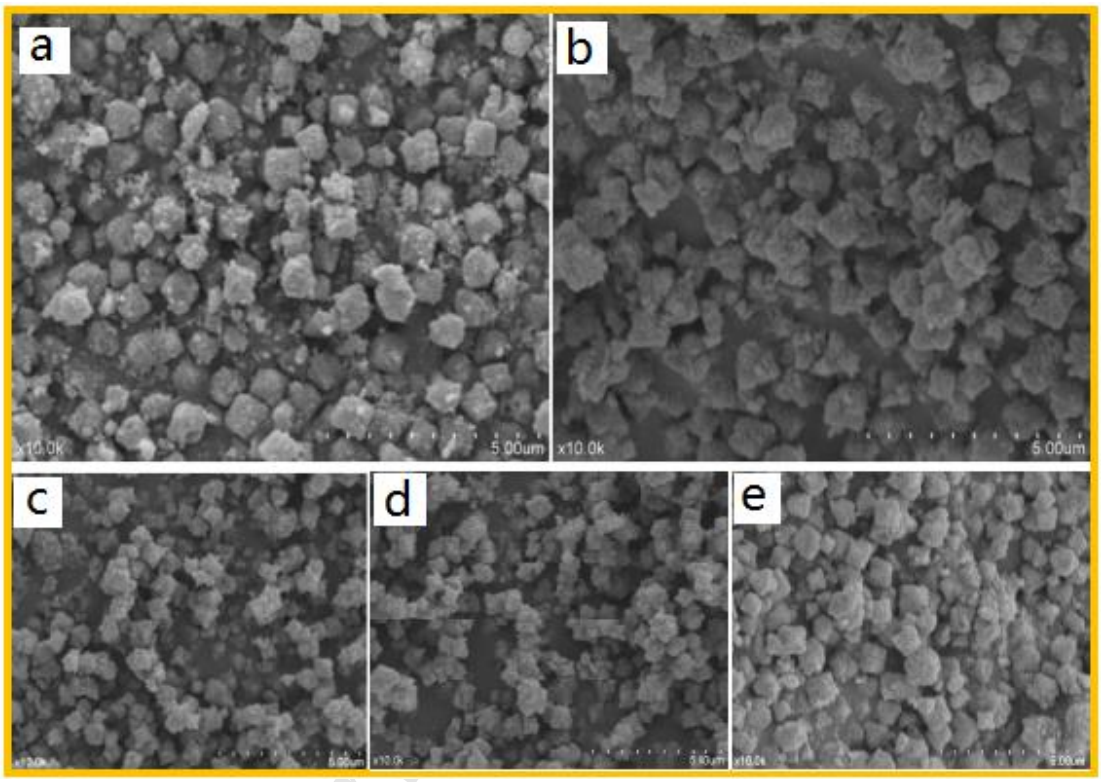

Fig.3

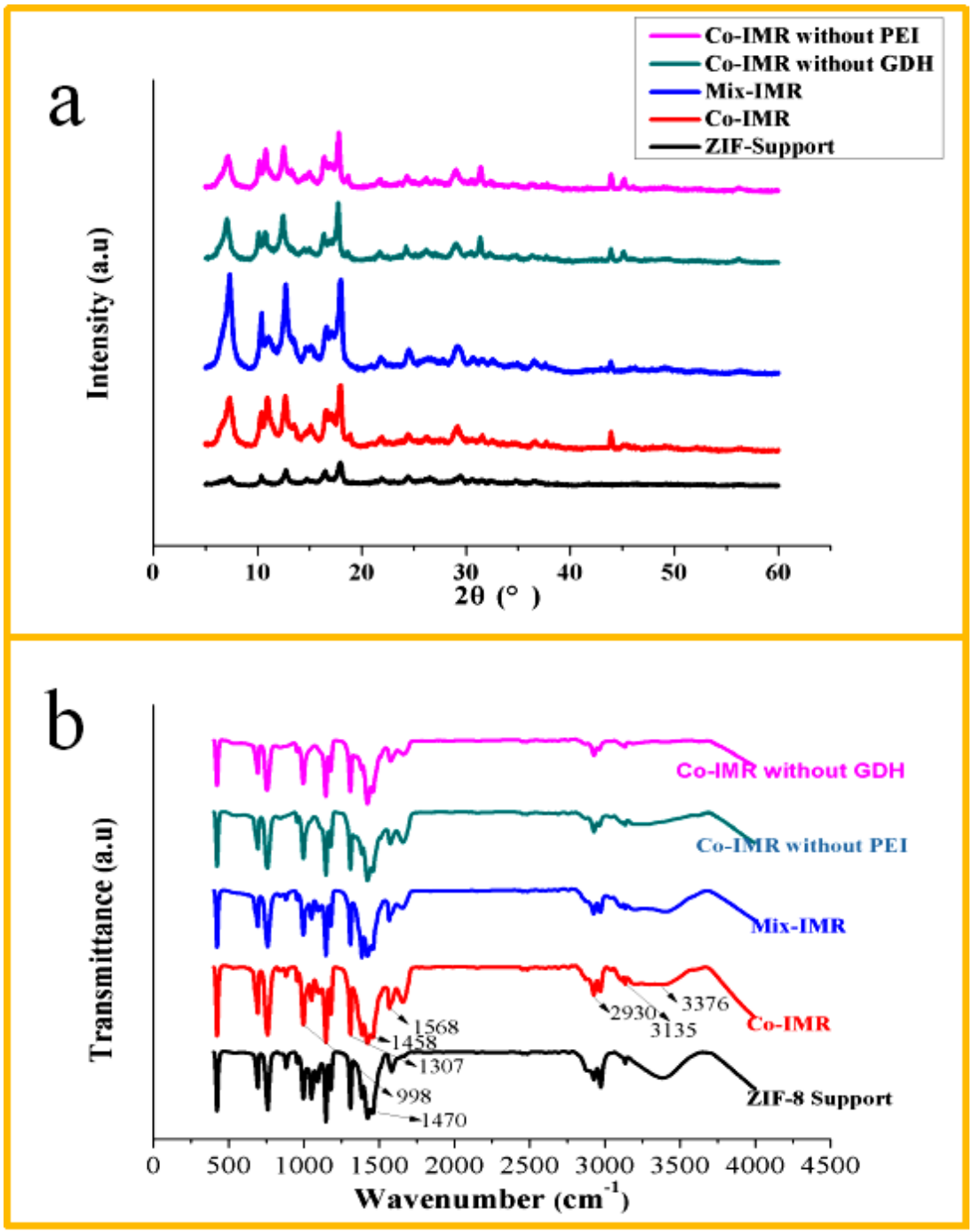
a
Co-IMR without PEI
Co-IMR without GDH
Mix-IMR
Co-IMR
ZIF-Support
Intensity (a.u)
0
10
20
30
40
50
60
2θ (°)
b
Co-IMR without GDH
Co-IMR without PEI
Mix-IMR
Co-IMR
ZIF-8 Support
Transmittance (a.u)
1568
1458
1307
998
1470
2930
3135
3376
0
500
1000
1500
2000
2500
3000
3500
4000
4500
Wavenumber (cm-1)

Fig. 4

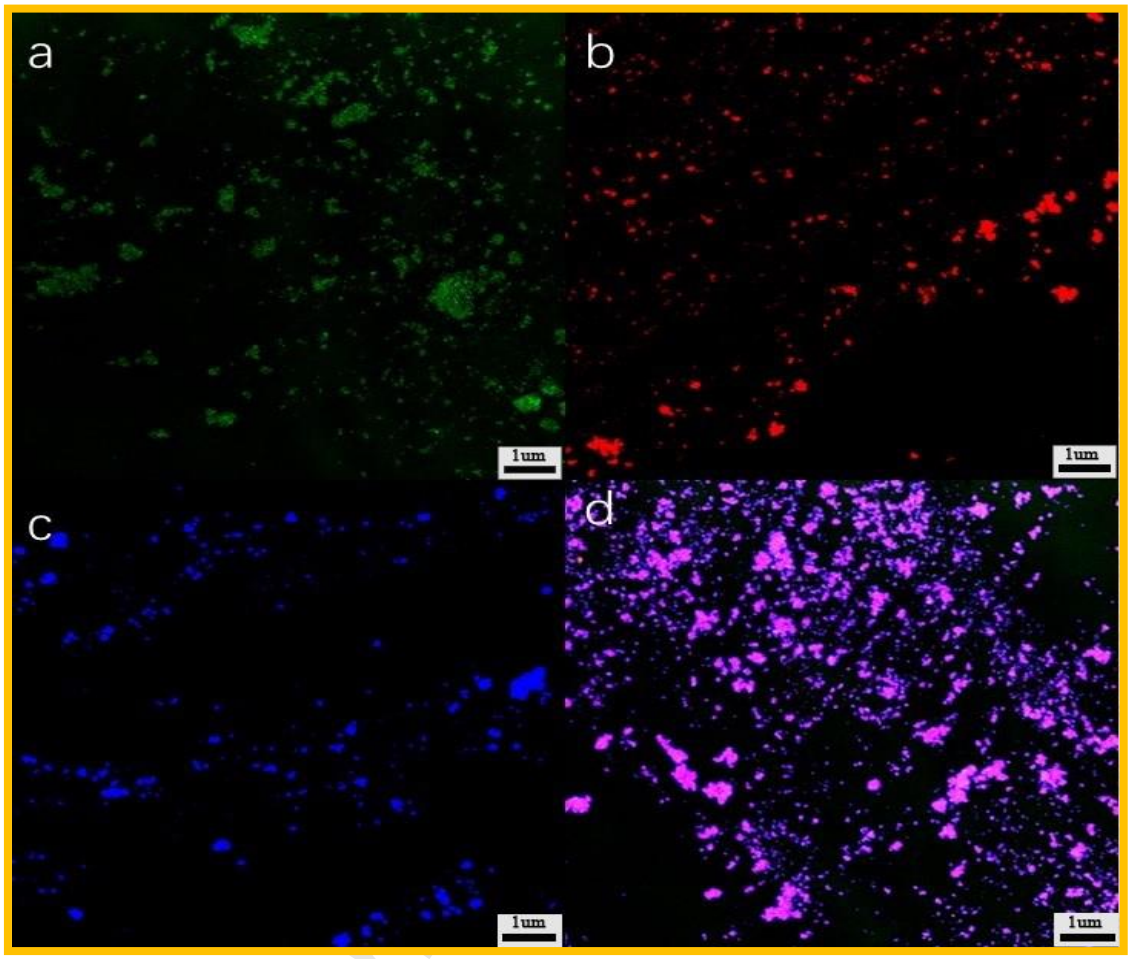

Fig. 5

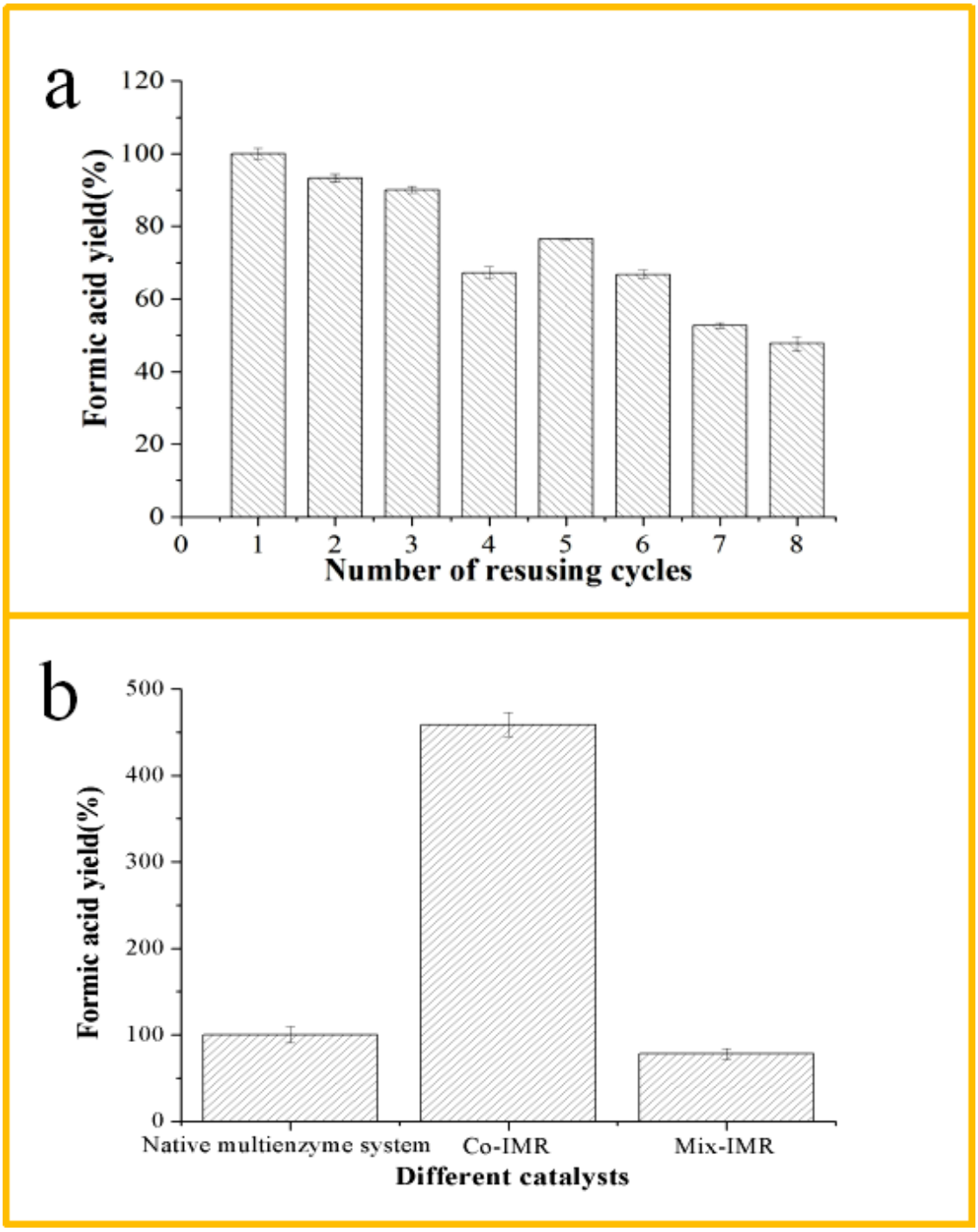
a
Formic acid yield(%)
120
100
80
60
40
20
0
0
1
2
3
4
5
6
7
8
Number of resusing cycles
b
Formic acid yield(%)
500
400
300
200
100
0
Native multienzyme system
Co-IMR
Mix-IMR
Different catalysts

Fig. 6

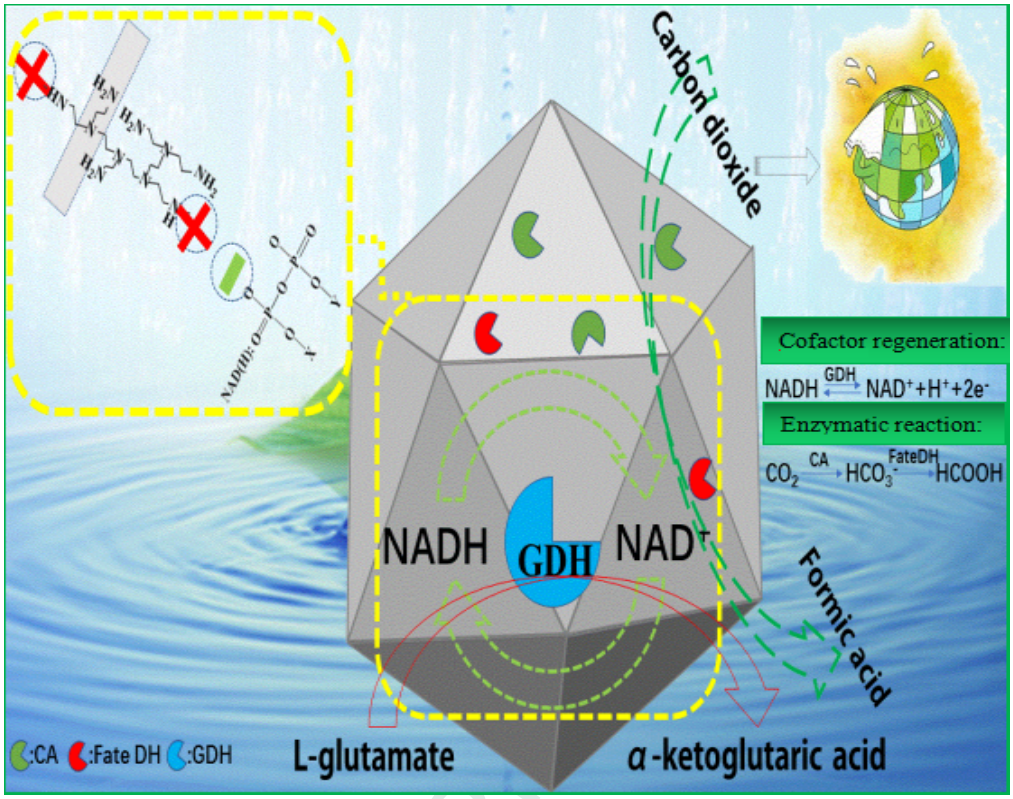

Graphical abstract

Highlights

- Nanoscale multienzyme reactor with cofactor regeneration for CO_2 conversion was constructed.
- Cofactor could be tethered in ZIF-8 via ion-exchange interactions between oppositely charged PEI and cofactor.
- The nanoscale multienzyme reactor exhibited superior capacity for conversion CO_2 to formate.